EXTRAPOLATING HOUSEHOLD LOAD DATA

Benedikt Eberl, FfE GmbH, +49 89 158121 – 47, beberl@ffe.de
Ferdinand Grimm, FfE GmbH
Michael Hinterstocker, FfE GmbH
Serafin von Roon, FfE GmbH

1 Overview

The integration of renewable energies is one of the major issues the energy sector is facing nowadays. In a system mainly supplied by conventional power stations, which are highly reliable in terms of time-dependent utilization, the principle of production following demand can easily be upheld. In a system which is characterized by a high degree of fluctuating feed-in, generation adequacy can either be reached by installing overcapacities on the supply side or by installing vast amounts of storage units, which allow for the bridging of temporal discrepancies between the demand and supply of electricity. The realization of these solutions seems unlikely because both solutions can lead to a surge in system costs. Hence, means of user-situated flexibility start moving into the centre of attention. This shall lead to a maxim where no longer production simply follows consumption, but consumption is also triggered by feed-in given by the conversion of non-dispatchable energy sources. Due to a fragmented and widespread distribution of energy production from renewables, a smart grid can help to control the system by enabling communication between all types of system elements. Such infrastructure is costly and not in all cases economically advantageous. A cost-benefit analysis of the Federal Ministry of Economics and Technology in Germany has concluded that the installation of smart meters in new and renovated buildings and in households/small businesses with a consumption superior to 6,000 kWh/a should be executed [1]. According to that, the Act on the Digitisation of the Energy Transition [2] has been adopted by the Bundestag in 2016. Within it, the Act of Metering Point Operation [3] has been issued. It decrees that from 2017 onwards, consumers with more than 10,000 kWh annual consumption and from 2020, users consuming more than 6,000 kWh/a have to be equipped with smart meters. Thus, only a share of the consumers in the grid are monitored, which results in an incomplete system coverage. Given the fact that most of the units producing electricity from renewable sources are situated in lower voltage levels of the electrical grid and new devices with high-level energy consumption like electric vehicles (EVs) or heat pumps are brought into the system, the supply situation in lower grid levels becomes more and more uncertain as standard load behaviour cannot be assumed. As in the German grid area-wide measurements are only conducted down to the 110 kV-level, most of the actions in the lower levels go unnoticed. With consumers more and more evolving to prosumers who interact with the electric system, knowledge about events taking place in lower grid levels become more and more important. As the consumption of households and their load profile has a major influence on lower grid levels, distribution network operators can benefit from knowledge of the load situation. Therefore, it is importan, that the development of the German power grid towards a smart grid will take a huge step forward, when the rollout of smart meters in Germany is carried out from 2017. As not all consumption will be measured, a method which allows aggregating selected household data to a reliable network load at different levels of the grid is required. This will help distribution network operators, energy providers and transmission network operators in forecasting their load situation. The presented approach thus aims to achieve a representative network load without knowledge of all household load data, as displayed in Figure 1.

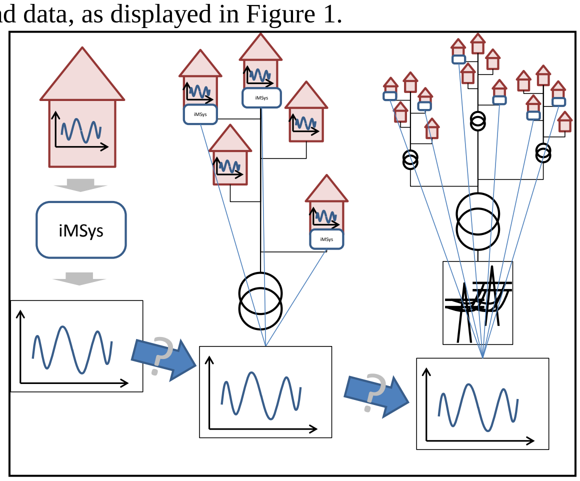

Figure 1: Extrapolation of single load data to line load data and to grid area data

This paper is a result of research in the project "C/sells – Das Energiesystem der Zukunft im Sonnenbogen Süddeutschlands – BASISmbH – Bayerische Systemintegration von Solarenergie" support code: "03SIN120" – fundet by the Fedeal Minestry for Economic Affairs and Energy.

2 Method

The main goal is to achieve valid network load synthesis by using single load profiles. To analyse the quality of the synthetic generation, mixed integer linear optimization (MILP) yields the optimal solution of a linear combination of *N* household profiles. As analyses have shown, MILP is in this case very time-consuming. Therefore, approaches that result in a less time-intensive process are discussed. This can be achieved by transforming the MILP into linear optimization (LP). By preselecting the most promising profiles for a synthetic generation of the network load, the mixed integer problem can be reduced to a linear problem.

Data of a total of *N* households is given over a timespan of $t \in [t_0, t_f]$. In regular time sampling intervals of the duration Δt, the consumed energy of the corresponding households within the previous interval is measured. Hereinafter the energy measured at the j-th sensor at the time instant $t_l = t_0 + l\Delta t$ is denoted as $L_j(t_l)$. Thus, the total number of samples for a certain household can be expressed as

$$T = \frac{t_f - t_0}{\Delta t}. \qquad (1)$$

The load recorded over time is stored in a vector $\hat{\boldsymbol{L}}_j$ for each of the *N* households:

$$\hat{\mathbf{L}}_j = \begin{bmatrix} L_j(t_0) & L_j(t_1) & \dots & L_j(t_T) \end{bmatrix}^T. \qquad (2)$$

In order to remove the influence of users with high energy consumption, each of the *N* recorded datavectors $\hat{\boldsymbol{L}}_j$ is then scaled to unit norm:

$$\mathbf{L}_j = \frac{\hat{\mathbf{L}}_j}{\|\hat{\mathbf{L}}_j\|_1}. \qquad (3)$$

The network load $L_S(t_l)$ at a certain time instant t_l is defined as the sum over the loads of all *N* households at t_l:

$$L_S(t_l) = \sum_{j=1}^{N} L_j(t_l). \qquad (4)$$

In order to find the network load $\boldsymbol{L}_S$ at all time instants, we define the following quantities:

$$\check{\mathbf{L}}_S = \begin{bmatrix} L_S(t_0) & L_S(t_1) & \dots & L_S(t_T) \end{bmatrix}^T, \qquad (5)$$

$$\mathbf{A} = \begin{bmatrix} L_1(t_1) & L_2(t_1) & \dots & L_N(t_1) \\ L_1(t_2) & L_2(t_2) & \dots & L_N(t_2) \\ \vdots & \vdots & \ddots & \vdots \\ L_1(t_T) & L_2(t_T) & \dots & L_N(t_T) \end{bmatrix}. \qquad (6)$$

Using $\check{\boldsymbol{L}}_S$ and $\boldsymbol{A}$ **,** the network load for all time instants is defined as the product between the auxiliary matrix A and an all-ones vector.

The goal is to express the network load using certain characteristic households. For this reason it is assumed that the network load can be approximated as a weighted sum of a subset of the households.

Therefore, the coefficients with which each of the households should be weighted are defined as

$$\mathbf{x} = \begin{bmatrix} x_1 & x_2 & \dots & x_N \end{bmatrix}^T. \qquad (7)$$

Based on the previously recorded data, an inverse model for the network load is obtained. The goal is to find the coefficients leading to the best approximation of the network load. This can be achieved by formulating and solving an optimization problem,

$$x^{opt} = \arg\min \|\check{\mathbf{L}}_S - \mathbf{A}\mathbf{x}\|_1 \quad \text{s.t.} \quad \|\mathbf{x}\|_0 \leq K. \tag{8}$$

The constraint enforces that only K entries of $\boldsymbol{x}$ are allowed to be nonzero. This constraint avoids that the all-ones vector will yield the optimal solution. The drawback of this formulation is that the above optimization problem is NP-hard to solve [4] since the position of the nonzero indices are not known beforehand. [4] further suggested to relax the optimization problem by replacing the sparsity operator with a linear norm. Detecting sparsity by minimizing the l_1-norm is a common solution for underdetemermined sparse minimization problems. However, in this case the problem is overdetermined. [5] showed that obtaining a sparse solution for an overdetermined minimization problem is difficult. For this reason the only method that could be applied in this case is the solution by exhaustive search. Therefore, a commercial solver such as CPLEX [6] can be used. In order to obtain an efficient solution it is thus necessary to reduce the dimensionality of the problem. This paper therefore analyses two aproaches to select the important load profiles by on the one hand examining their function properties and on the other hand an analysis of their frequencies. As soon as the position of the nonzero coefficients is known, it is possible to shrink $\boldsymbol{A}$ by removing each column of a non-used profile. The remaining coefficients can then be computed by solving the minimization problem without the constraint.

2.1 Sorting profiles by central moments

In order to find which of the given loads $\boldsymbol{L_j}$ is a candidate to represent the network load, we examine the behaviour of the function of their energy consumption over time. As each of the single loads is non-negative and their sum is normalized to 1, they describe valid probability distributions, even though the interpretation is different in this case. For this reason, we aim to examine the statistical properties of each of the load profiles and compare it to the properties of the normalized network load,

$$\mathbf{L}_S = \frac{\check{\mathbf{L}}_S}{\|\check{\mathbf{L}}_S\|_1}. \tag{9}$$

This ensures that the sum of the network loads over the timesteps is scaled to 1. In this way, the network load can also be interpreted as a valid probability distribution.
To describe probability distribution functions, their central moments can be used. The central moments $\boldsymbol{\mu_n}$ of an arbitrary probability distribution function $\boldsymbol{X}$ are given as [7]:

$$\mu_n = \mathrm{E}[\mathbf{L} - \mathrm{E}[\mathbf{L}]^n]. \tag{10}$$

The first central moments have an interpretation that can be seen on the plot of the probability distribution function:

- The first central moment $\boldsymbol{\mu_1}$ is always 0. Therefore, it is not considered in this paper.
- The second central moment $\boldsymbol{\mu_2}$ is the variance of the distribution which is related to the deviation of the distribution from the mean.
- The third central moment is the (non-) normalized skewness of the distribution. It can be interpreted as an indicator for the symmetry of the distribution.
- $\boldsymbol{\mu_4}$ is known as the non-normalized kurtosis of $\boldsymbol{X}$.

Since the goal is to find a concrete number of household profiles which are related to the sum of the load profiles, the first P central moments $\boldsymbol{\mu_n}(\boldsymbol{L_j})$ of all the recorded load profiles are computed. Furthermore, the first P central moments of the network load are calculated to allow comparing the single load profiles to the network load. In the next step, the n-th root of the central moments is taken and scaled to the n-th central moment of the network load. Hence, it is possible to combine different moments using linear algebra. To be able to select different load profiles, the delta of the moments of the single load profiles and the moments of the network load is calculated. The selection is made by sorting the delta values. Afterwards, the scalar values for minimizing the error are calculated using linear optimization. Therefore, an unconstrained optimization problem can be solved, taking only the selected loads into account:

$$x^{opt} = \arg\min \|\check{\mathbf{L}}_S - \mathbf{A}\mathbf{x}\|_1. \tag{11}$$

2.2 Approximation with integral transformations

From an intuitive point of view, the energy consumption is dominated by periodically recurring events. Load profiles can be used to summarize large scale observations because consumers exhibit habitual behaviour. These intuitive findings can be used to design a framework that compresses the information about our energy consumption to a fraction of the original. Since the energy consumption seems to be related to periodic processes, it might be beneficial to take this behaviour into account. Therefore, the time-based load profiles are transformed into the frequencies, a fraction of the main frequencies is cut out and a distinct number of profiles is selected using mixed integer linear optimization. Having selected the most important profiles, linear optimization can be conducted for the original profiles using only the selected single load profiles. Two different types of transforms are analysed, the discrete fourier transform and the discrete cosine transform.

2.2.1 Discrete fourier transform-based approximation

The idea of applying the Fourier transform in order to reduce computational cost is widely used. Among the most popular examples is the FFT-based convolution [8], [9]. The main goal of this section is to define a computationally efficient Fourier transform based framework for the approximation of sumloads

From a mathematical point of view, all continuous periodic signals f(t) can be described with their inverse Fourier transform

$$f(t) = \int_{-\pi}^{\pi} \tilde{f}(\omega)\exp(i\omega t)\mathrm{d}\omega, \qquad (12)$$

where i denotes the imaginary unit. The fourier transform $\hat{f}$ can be obtained as the integral of the product of the signal f(t) and the complex conjugate of the corresponding basis function:

$$\tilde{f}(\omega) = \frac{1}{2\pi}\int_{-\pi}^{\pi} f(t)\exp(-i\omega t)\mathrm{d}t. \qquad (13)$$

In the case of the network load approximation a continuous system is not available. In order to obtain similar results, we apply the discrete fourier transform (DFT) on the load profiles as well as the network loads instead.

Given a sampled signal L_t, consisting of T samples, the discrete fourier transform is given as

$$\mathbf{l}'_k = \sum_{t=0}^{T-1} \mathbf{L}_t \exp\left(\frac{2\pi ikt}{T}\right). \qquad (14)$$

The resulting signal l'_k is a vector of length N. An efficient algorithm to compute the DFT is the fast fourier transform (FFT) which was introduced by Cooley and Tukey [10]. l'_k is also referred to as the frequency domain representation of L_t. For the time domain representation, the inverse DFT on the frequency domain representation is used.

$$\mathbf{L}_t = \sum_{k=0}^{T-1} \mathbf{l}'_k \exp\left(\frac{2\pi ikt}{T}\right). \qquad (15)$$

It should be noted that $l'_k$is a complex signal while the original signal L_t which describes the load is real. For this reason, the DFT of L_t will be symmetric around $k = \frac{T}{2}$. Since those values of l'_k which correspond to $k > \frac{T}{2}$ do not give any new information, they shall be removed in order to reduce the computational complexity and memory consumption:

$$\bar{\mathbf{l}}'_k = \mathbf{l}'_k\left(1 : \frac{T}{2}\right). \qquad (16)$$

The notation $l(a{:}b)$ implies that all entries of the vector l with indices between a and b are considered. Furthermore, some commercial optimization packages do not support the usage of complex data. For this reason, it is necessary to create a real-valued data set. A possible solution for this is to stack real- and imaginary part of the obtained vector:

$$\mathbf{l}_{k,\text{stacked}} = \begin{pmatrix} \Re(\bar{\mathbf{l}}'_k) \\ \Im(\bar{\mathbf{l}}'_k) \end{pmatrix}. \qquad (17)$$

The advantage of this method is that the full information of the signal can be used by a real-valued solver in this way. However, the complexity compared to the original problem increases again.

Therefore, another method is utilized here. Every complex number can be described by magnitude $|x|$ and phase $\varphi(x)$ as well:

$$
\begin{aligned}
|\bar{\mathbf{l}}'_k| &= \sqrt{\Re({}^{\prime}\bar{\mathbf{l}}_k)^2 + \Im({}^{\prime}\bar{\mathbf{l}}_k)^2} && (18) \\
\varphi(\bar{\mathbf{l}}') &= \arctan\left(\frac{\Im(\bar{\mathbf{l}}'_k)}{\Re(\bar{\mathbf{l}}'_k)}\right). && (19)
\end{aligned}
$$

While the magnitude contains the information of the amplitude of each basic function of the DFT, the phase gives insight about the initial value of the corresponding basic function. In the case of network load approximation, each signal is recorded in parallel over a year. Many external factors for the energy consumption are depending on the time of the day, the season, or the weather.

Since those events are similar to all users, and since the recording for all loads started at the same time, the phase differences are assumed to be negligible. For this reason, only the magnitude of the DFT signal is taken into account:

$$
\mathbf{l}_k = |\bar{\mathbf{l}}'_k|. \qquad (20)
$$

In order to obtain an approximation for the network load, the DFT of each load $l_{k,j}$ is computed and the network load $l_{k,s}$respectively. After that, the symmetric part is cut off and the magnitude of the remaining signals is calculated. The goal is to find a linear combination of some of the individual loads which yields an approximation for the network load.

Since the DFT as well as the inverse DFT are linear, a linear combination of M loads in the frequency domain can be straightforwardly transformed to the corresponding linear combination of loads in the time domain:

$$
\begin{aligned}
\mathbf{l}_S &\approx \sum_{m=0}^{M} x_m \mathbf{l}_m && (21) \\
\sum_{k=0}^{T-1} \mathbf{l}_{S,k} \exp\left(\frac{2\pi ikt}{T}\right). &\approx \sum_{k=0}^{T-1} \left(\sum_{m=0}^{M} x_m \mathbf{l}_{m,k}\right) \exp\left(\frac{2\pi ikt}{T}\right) \\
\mathbf{L}_S &\approx \sum_{m=0}^{M} x_m \left(\sum_{k=0}^{T-1} \mathbf{l}_{m,k} \exp\left(\frac{2\pi ikt}{T}\right)\right) \\
&\approx \sum_{m=0}^{M} x_m \mathbf{L}_m && (22)
\end{aligned}
$$

For this reason, the whole optimization problem can be solved in the frequency domain instead of the time domain. Since the frequency domain representation of the load only has half of the length of the corresponding time domain representation, the complexity of the optimization problem will be reduced by a half.

However, it is possible to reduce the complexity of the framework even further. While each sample in the time domain seems to be equally important to represent the complete load, this is not true for the frequency domain. In fact, most frequencies seem to have very little influence and just represent some kind of noise that can be interpreted as small deviations from the daily routine of consumers. In order to further reduce the computational complexity, those frequencies are neglected. **Figure 3** shows part of the magnitude of the FFT of the network load.

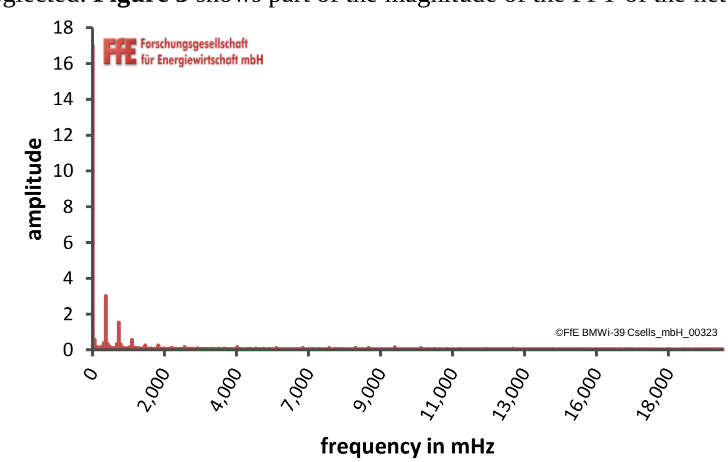

Figure 3: FFT of the network load

It seems obvious that only a small fraction of the frequencies are relevant. Thus, for the optimization only those frequencies with the highest magnitudes of the network load shall be matched. In this way, a major reduction of the computational complexity is achieved. The framework is summarized in **Figure 4**.

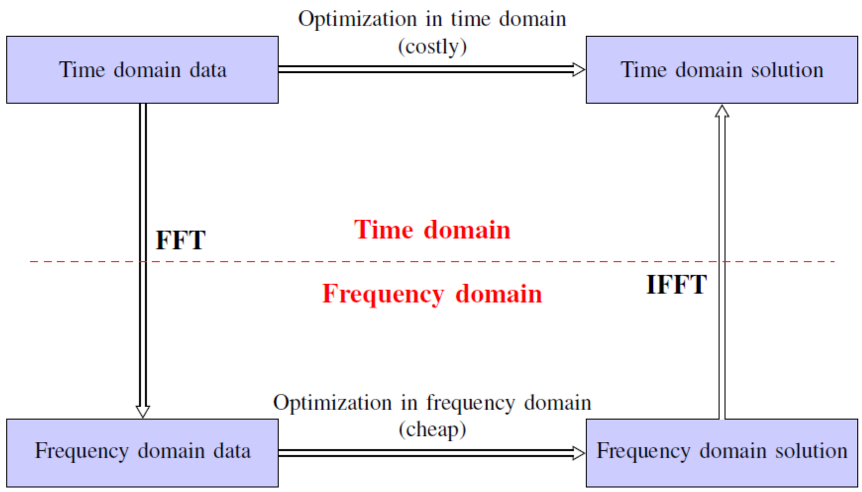

Figure 4: Framework of selection load profiles using FFT

2.2.2 Discrete cosine transform-based approximation

The discrete cosine transform (DCT) [11] is another often used transformation. It is mainly used in in image processing due to its compressive nature. The most common application of the discrete cosine transform today is the JPEG data format [12]. Another advantage of the discrete cosine transform is that the output is real-valued, contrary to the DFT, where a complex output is generated.The approach presented in this section is similar to the approach of the previous section with using the DCT instead of the DFT. The goal is to improve the performance by not removing the phase information when only taking the magnitude of the DFT. At the same time, the computational complexity shall remain the same. The type 2 discrete cosine transform of a sampled signal is given by[13]:

$$\mathbf{l}_k = \sum_{t=0}^{T-1} \mathbf{L}_t \cos\left(\frac{\pi}{T}(t+0.5)k\right). \qquad (23)$$

Similarly to the DFT, the DCT is linear. This allows to transfer the framework from the previous section to the DCT. The only differences are that for the DCT, the data does not need to be prepared by cutting off symmetric values or disregarding the phase. Furthermore, efficient algorithms for computation of the DCT can be found for example in [14] or [15].

3 Results

The different approaches lead to very different results. In this paper, a comparison between the optimal solution for the total error, represented by the sum of the absolute errors of every timestep, using mixed integer linear optimation for a linear combination of 5 and 10 selected load profiles is displayed. The optimal solution already has been calculated and discussed in [16]. In Figure 5, the error distribution is shown for all permutations of linear combinations of 5 (left) and 10 (right) profiles.

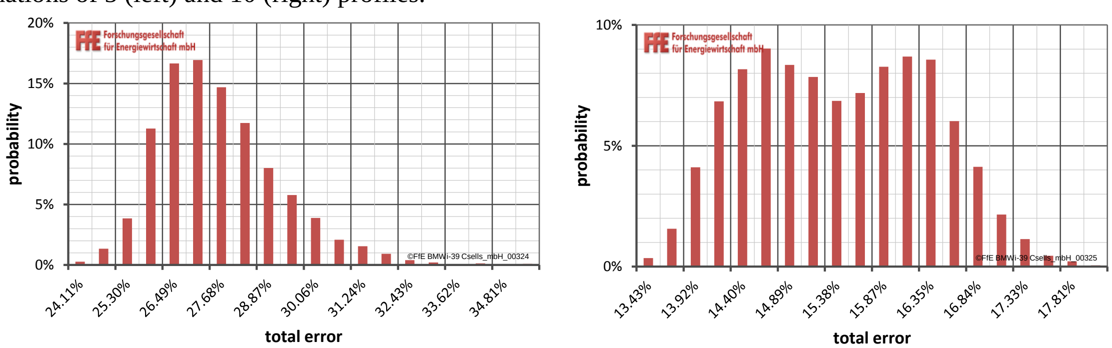

Figure 5: Error distribution for linear combinations of 5 (left) and 10 (right) profiles

3.1 Results: Sorting profiles by central moments

This approach allows to select load profiles depending on their central moments. In a first analysis, the central moments number 2 to 11 were calculated. Two different ways of finding criteria for the selection of the important profiles shall be displayed in this paper. Firstly, the selection is conducted regarding the ranking of the delta between all moments of the single profiles and the moments of the network load. Secondly, the cumulated sum of the moments from moment 2 to *n* is analysed. Figure 6 displays the results for all numbers of used profiles and all regarded moments.

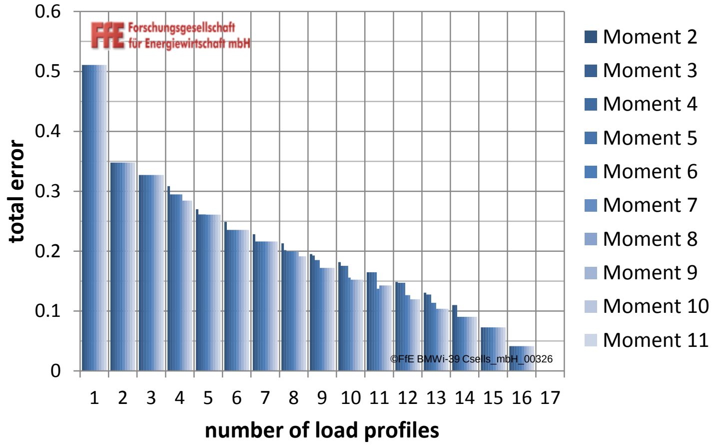

Figure 6: Total error using the central moments 2 to 11 and 1 to 17 allowed profiles

The figure reveals that the smallest delta between single profiles and the network load is reached by the same profile when using 1 to 3 profiles. Only regarding more than 3 profiles in the linear combination lead to a different choice of profiles for different moments. It seems as if higher moments lead to a smaller total error. Comparing the total value of the error to the error distribution reveals that for a linear combination of 5 load profiles, the smallest error is 26.10 %. The error for 10 load profiles is 15.23 % None of the central moments lead to a total error that does seem promising. Nevertheless, the sum of all moments could lead to another result. Therefore, Figure 7 shows the error if the selection is done by sorting the cumulated sum of the central moments 2 to 11 for 1 to 17 allowed profiles.

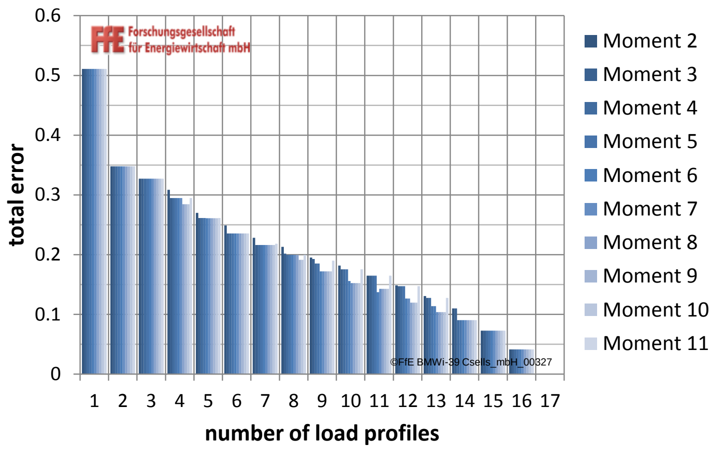

Figure 7: Total error using the cumulated sum of the central moments 2 to 11 and 1 to 17 allowed profiles

The figure shows small differences compared to Figure 6. The minimal error of the combinations of 5 and 10 load profiles is higher than it is for only using the moments without any modifications. It is 26.12 % for 5 profiles and 17.55 % for 10 profiles, which is among the highest errors possible regarding the error distribution.

3.2 Approximation with integral transformations

The idea of using transforms into the frequency domain is based on personal behaviour regarding energy consumption. These behavioural habits should be reflected in the electric load profiles. If important frequencies can be filtered, the mixed integer optimization (MILP) of the reduced FFT is faster as the number of lines in the matrix containing all transforms of load profiles is reduced.

In a first run, the FFT of the data was computed, where only the main frequencies where optimized using MILP. Figure 8 shows the total error for different fractions of used frequencies for linear combinations of 5 and 10 profiles, where the result of the optimization in the frequency domain is used.

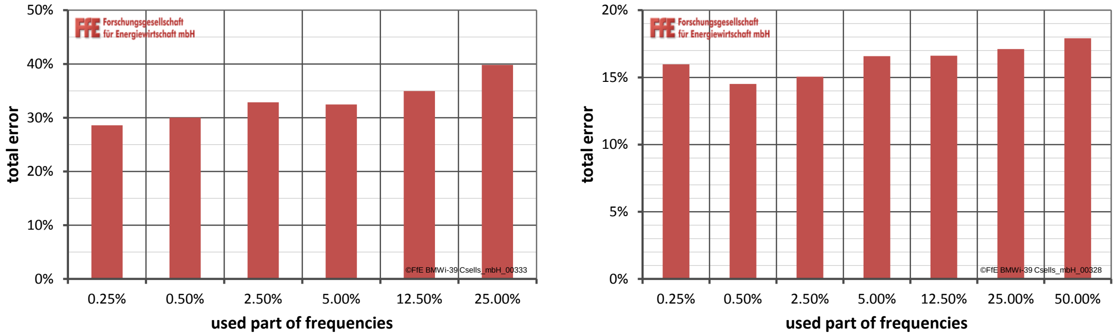

Figure 8: **Total error (time-based) of frequency optimization using 5 (left) and 10 (right) profiles for different used parts of frequencies after FFT**

The figures show that the error after the optimization in the frequency domain is higher for a higher number of used frequencies. As the main goal of the transform was to identify the important profiles and not to solve the optimization problem, the LP with the selected profiles was performed in the time domain. In Figure 9, the total error of the time-based optimization using the selected profiles from the optimization in the frequencies can be seen for different parts of frequencies.

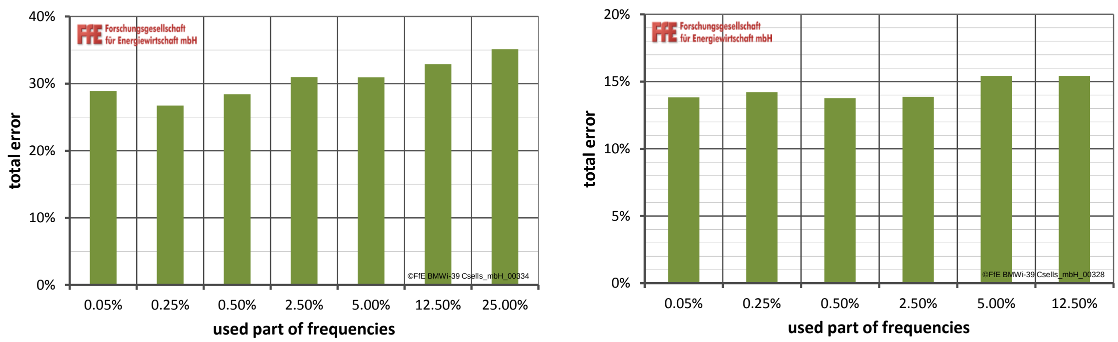

Figure 9: **Total error (time-based) of time-based optimization using 5 (left) and 10 (right) profiles for different used parts of frequencies after FFT**

The figure shows that with LP in time domain, the fact that smaller parts of frequencies are beneficial for the selection of important profiles is maintained. Regarding the total error evinces that for 5 (10) profiles, the minimal error can be reduced from 28.6 % (14.5 %) to 26.7 % (13.8 %). To find the range where the overall minimum error can be seen, a detailed analysis is carried out for the range from 0.05 % to 2.5 % as it can be found in Figure 10.

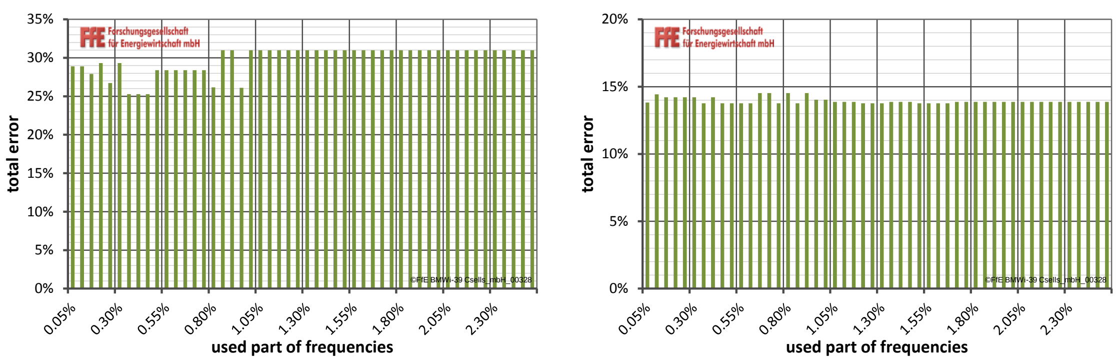

Figure 10 **Total error (time-based) of time-based optimization using 5 (left) and 10 (right) profiles for different used parts of frequencies after FFT**

Regarding the total errors for 5 (10) selected profiles, a minimal error of 26.7 % (13.8 %) can be found for 0.45 % (0.45 % to 0.60 %) selected frequencies. That equals to 158 frequencies when using data over one year with a resolution of 15 minutes.

The same method was repeated for the discrete cosine transform (DCT). At first, the main frequencies were selected with a MILP. Figure 11 displays the time-based error after optimization in the frequency domain using 5 (left) and 10 (right) profiles.

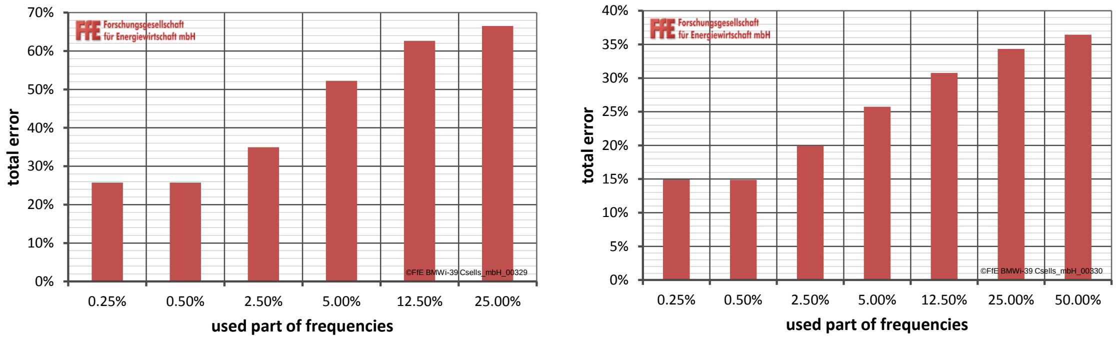

Figure 11: **Total error (time-based) of frequency optimization using 5 (left) and 10 (right) profiles for different used parts of frequencies after dct**

It can be seen that the time-based error of the frequency optimization is higher for higher shares of frequencies utilized. Using the selection of profiles in the time domain for LP results in the error shown in Figure 12.

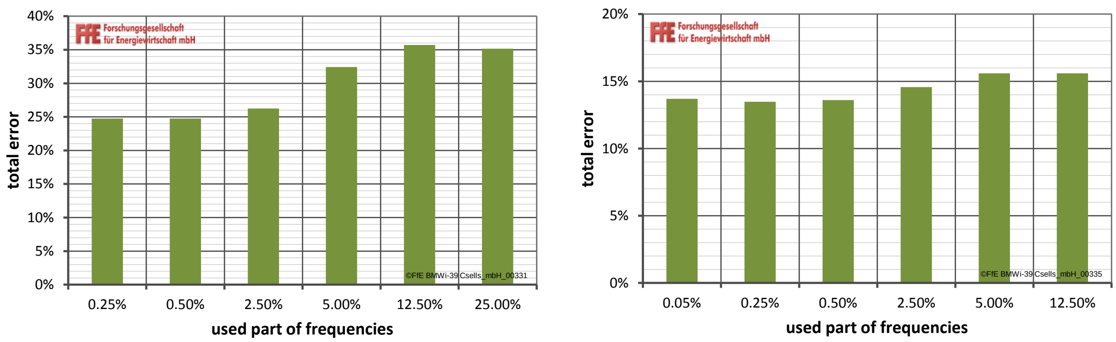

Figure 12: **Total error (time-based) of time-based optimization using 5 (left) and 10 (right) profiles for different used parts of frequencies after dct**

The graphics show that a minimum for the error can be found when using between the best 0.05 % and 2.50 % of the frequencies. Therefore, a detailed analysis of this range is conducted and displayed in Figure 13.

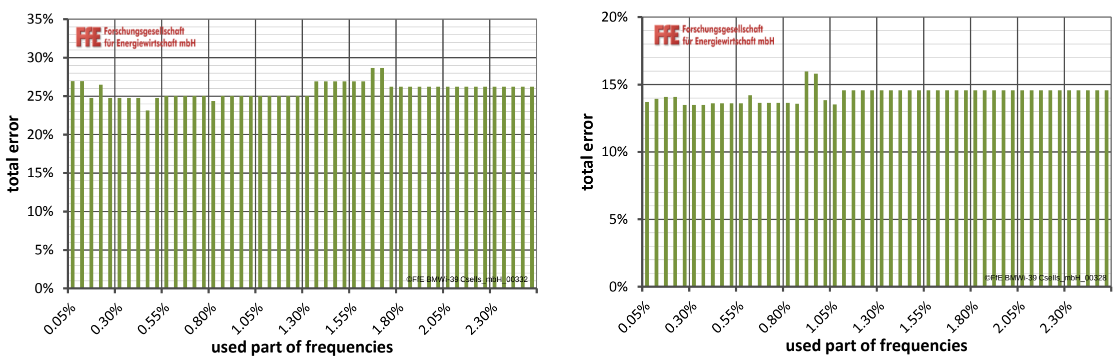

Figure 13: **Total error (time-based) of time-based optimization using 5 (left) and 10 (right) profiles for different used parts of frequencies after dct**

As seen before regarding the results of the FFT-based selection, the smallest error with 23.1 % (13.5 %) can be found using the best 0.45 % (0.25 % to 0.35 %) of the frequencies for 5 (10) selected profiles.

4 Conclusions

In this paper, different approaches to select representative profiles to recreate a network profile have been introduced. In a first approach, a selection of the profiles was performed using the central moments of the time series as a statistical characterization of themselves. It can be seen that different combinations of the multiple central moments as criteria did not lead to better results.

In a second approach, the time-based problem was transformed into the frequency domain to reduce the problem. The idea is, that due to periodical behaviour of consumers, not all frequencies have the same importance. Therefore, two transforms are tested. The discrete fourier transform and the discrete cosine transform were used. The latter does not have an imaginary output as a result. It can be seen that reducing the problem down to 0.45 % of the frequencies for the linear combination of 5 profiles and down to 0.25 % of the frequencies for the combination of 10 profiles produces the best results. In Figure 14, the distribution of the minimum errors is displayed and the results that could be found with the different approaches are located in the corresponding range.

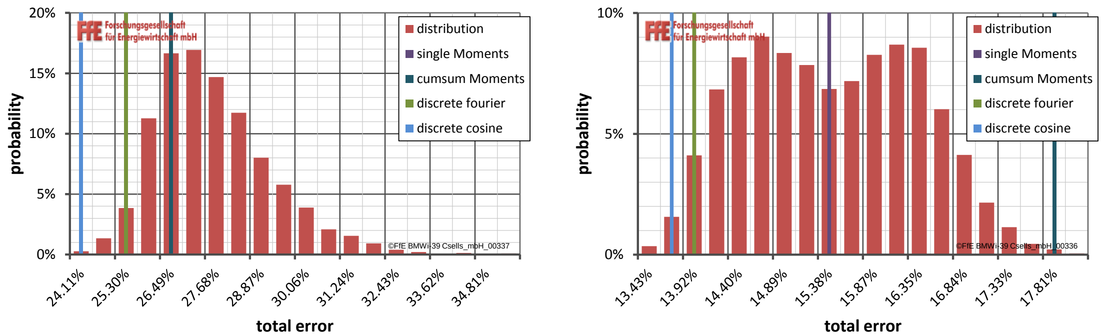

Figure 14: Distribution of errors and location of the results obtained by the different approachs

The figures show that due to reduction of the problem in the frequency domain to 0.25 % of the initial problem, adequate results can be obtained. Hereby, the discrete cosine transform evinces better results than the discrete fourier transform.

5 References

[1] Kosten-Nutzen-Analyse für einen flächendeckenden Einsatz intelligenter Zähler - Endbericht zur Studie im Auftrag des Bundesministeriums für Wirtschaft und Technologie. Stuttgart: Ernst & Young GmbH, 2013

[2] Gesetz zur Digitalisierung der Energiewende. Berlin: Bundesregierung, 2016

[3] Messstellenbetriebsgesetz - Gesetz über den Messstellenbetrieb und die Datenkommunikation in intelligenten Energienetzen . Berlin: Bundesministerium der Justiz und für Verbraucherschutz, 2016

[4] Donoho, David L. "Compressed sensing." IEEE Transactions on information theory 52.4 (2006): 1289-1306.

[5] Guruswami, Venkatesan, and Prasad Raghavendra. "Hardness of solving sparse overdetermined linear systems: A 3-query PCP over integers." *ACM Transactions on Computation Theory (TOCT)* 1.2 (2009): 6.

[6] IBM ILOG, Inc. *CPLEX 12.5 User Manual*. Somers, NY, USA, 2012.

[7] Menascé, Daniel A. : Probability and Discrete Probability Distributions. Fairfax: Department of Computer Science George Mason University, 2001

[8] Burrus, C. Sidney, and T. W. Parks. "DFT-FFT and Convolution Algorithms: theory and implementation." John Wiley and Sons, New York, 1985.

[9] Agarwal, R. C., and C. Burrus. "Fast convolution using Fermat number transforms with applications to digital filtering." IEEE Transactions on Acoustics, Speech, and Signal Processing 22.2 (1974): 87-97.

[10] Cooley, James W., and John W. Tukey. "An algorithm for the machine calculation of complex Fourier series." Mathematics of computation 19.90 (1965): 297-301.

[11] Ahmed, Nasir, T_ Natarajan, and Kamisetty R. Rao. "Discrete cosine transform." IEEE transactions on Computers 100.1 (1974): 90-93.

[12] Wallace, Gregory K. "The JPEG still picture compression standard." IEEE transactions on consumer electronics 38.1 (1992): xviii-xxxiv.

[13] Strang, Gilbert. "The discrete cosine transform." SIAM review 41.1 (1999): 135-147.

[14] Chen, Wen-Hsiung, Smith, C. H. and Fralick, S. C.. "A fast computational algorithm for the discrete cosine transform." IEEE Transactions on communications 25.9 (1977): 1004-1009.

[15] Lee, Byeong. "A new algorithm to compute the discrete cosine transform." IEEE Transactions on Acoustics, Speech, and Signal Processing 32.6 (1984): 1243-1245.

[16] Eberl, Benedikt, Hinterstocker, Michael and von Roon, Serafin - „Von Smart-Meter-Daten zum Netzlastgang“, Conference paper, IEWT Wien 2017, Wien